JOURNAL OF OPTOELECTRONICS AND ADVANCED MATERIALS Vol. 10, No. 10, October 2008, p. 2574 - 2577

Ethanol sensing performances of modified $CoFe_2O_4$ nanocrystals prepared by polymerizable complex route

G. N. CHAUDHARI, M. J. PAWAR*
Nanotechnology Research Laboratory, Shri Shivaji Science College, Amravati M.S., India

Spinel compound, $CoFe_2O_4$; an n-type semiconducting metal oxide has been synthesized by polymerizable complex route and characterized by X-ray diffraction (XRD) and scanning electron microscopy (SEM). The sensitivity of $CoFe_2O_4$ thick films was measured at different operating temperatures. Ethanol detection results of sample GII show peak sensitivity at 150^0C. The variation of sensitivity and ethanol concentration has shown an increase in sensor response and get saturated at 600 ppm. Sample GII impregnated with 1 wt.% palladium was able to detect 100 ppm of ethanol at 100^0C. A low temperature ethanol sensitivity of $CoFe_2O_4$ is attributed due to polymerizable complex method employed for material preparation and impregnation of noble metal.

(Received December 26, 2007; accepted August 14, 2008)

Keywords: Nanomaterials; $CoFe_2O_4$; Ethanol; Sensitivity; Palladium

1. Introduction

In the present era, environmental security has become more important globally. A lot of attention has been paid to the development of solid-state devices for detection of toxic gases in air. Semiconductor gas sensors can be used for this response since they can detect various toxic gases by changing its conductivity due to the adsorption and/or desorption of the metal oxide surface. The majority of the works done on the gas sensitive nanocrystalline semiconductor oxides aim to improve the functional parameters; selectivity and response. Although a large number of different oxides have been investigated for their gas sensing properties in the form of thick film, thin film and pellets. Fine metal oxide powders for sensing applications have been produced by several methods, including sol-gel processing [1], spray pyrolysis [2], pulsed laser ablation [3], chemical vapor deposition [4], sputtering [5] and thermal decomposition [6,7].

In a previous paper we reported on the sensing properties of perovskite $Bi(Fe,Mn)O_3$ ferrite toward liquid petroleum gas detection [8].

In solid-state sciences, the oxides with spinel structure (e.g. $NiFe_2O_4$, $ZnFe_2O_4$, etc) are some of the most studied compounds due to their wide range of applications. The structure of spinel oxide is responsible for a variety of interesting properties [9-13]. $CoFe_2O_4$ is expected to have sufficient thermodynamic stability and perfect sensing properties. CoO and Fe_2O_3 have been used in development of gas sensors from decades due to their high sensitivity. Nanocrystalline $CoFe_2O_4$ system offers a great potential as magnetic materials [14-16] and also as catalysts [17].

The goal of this investigation is to present an alternative method to produce fine $CoFe_2O_4$ nanocrystals with controlled electrical properties for subsequent C_2H_5OH sensor applications.

2.Experimental

2.1 Synthesis of $CoFe_2O_4$ nanocrystals

$CoFe_2O_4$ compounds were obtained by a polymerizable complex method. In the aqueous solution of citric acid (CA), cobalt nitrate and ferrous nitrates were added in stoichiometric ratio. The mixture was kept on a magnetic stirrer at 70^0C for 4 hr in order to get stable metal-CA complex. The resultant solution was then added with an appropriate amount of ethylene glycol (EG) and was stirred continuously for 7 hr at 90^0C for removal of extra water. While stirring, a resin like mass is formed by polyesterification between CA and EG. Heating in the range of temperature from 350-400^0C decomposed the polymeric resin. The decomposed resin was treated in a mantle heater at 400-450^0C over 3 hr in order to evaporate highly combustible species and induce charring. So formed ash was slightly ground in to powder and calcined at 500^0C (Sample GI), 600^0C (Sample GII) and 700^0C (Sample GIII) each for 6 hr.

2.2 Palladium incorporation over $CoFe_2O_4$ compound

Palladium was impregnated in the $CoFe_2O_4$ nanomaterials by a chemical wet impregnation route. Appropriate quantities of $PdCl_2$ and samples were dissolved in deionized water followed by the vigorous stirring and slow drying in a water bath. The dried compound was ground to a fine powder and calcined at 300^0C for 2 hr for decomposition of chlorides.

2.3 Sensing measurements

Thick-film gas sensors were prepared by conventional hand coating of a paste; the nano $CoFe_2O_4$ powders were mixed with a α-terpineol based solvent, over the 0.2 mm gap of gold electrodes on a 7×8 mm Al_2O_3 substrate. Subsequently, these substrates were sintered at 700 °C for 1 hr in air. Platinum wires were attached to the pads of the heater and sensing electrodes by using an Au-paste and heat treatment. Sensors to be tested were placed in a measuring chamber of about 0.5 dm^3 in volume. Optimum detection temperatures were determined and thick-film sensors maintained at this fixed temperature. Were exposed to reducing gases like C_2H_5OH, CO, CH_4 and LPG using a gas flow controller unit with an air flow rate of 0.5 dm^3/min. Response, S to gas is defined as

$$S = R_{(air)} - R_{(gas)} / R_{(gas)}$$

where, $R_{(air)}$ and $R_{(gas)}$ are the resistance of sensor in clean air and in the test gas respectively.

3. Result and discussion

3.1 Characterization

The materials were characterized by XRD using a Siemens D5000 diffractometer and Cu Kα radiations (1.5406Å0). The X-ray diffraction confirmed that all the samples are monophasic. Fig.1 shows the XRD pattern at room temperature for the $CoFe_2O_4$ compounds calcined in the range of 600 °C (sample GII). All the diffraction peaks corresponds to cubic spinel structure. The broadening of different peaks indicates that the particles are of nanometer scale and the average particle size was found to be 60-40 nm.

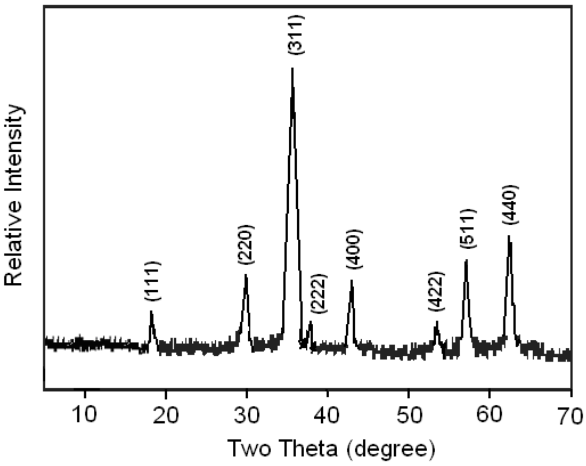

Fig.1. XRD pattern of $CoFe_2O_4$.

The microstructure of the sample can be visualized from scanning electron micrograph (SEM) of the synthesized materials as in Fig. 2. The presence of macro agglomerations containing very fine particles (under 4 μm) can be observed. The particle shapes are not well defined. Many large and small pores are present in the whole material. It was assumed that the pores mainly intergranular because such pores are not observed on the SEM photograph.

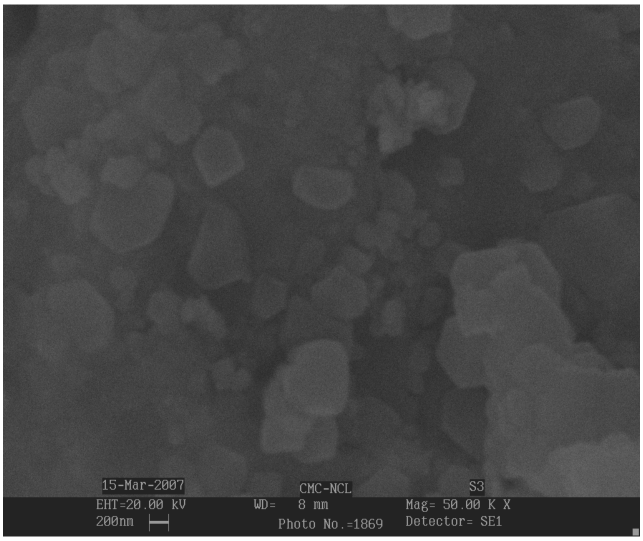

Fig. 2. SEM micrograph of sample GII.

3.2 Gas sensing characteristics of $CoFe_2O_4$

Fig. 3 shows the gas sensitivity for all the samples in the presence of the ethanol vapors, at various temperatures. The gas sensitivity usually depends on the sensor operating temperature, particle size and addition. It is evident that the sensitivities vary with the increase and decrease of particle size of sensor. As seen in Fig. 3, sample GII show high sensitivity to ethanol at 150^{0}C. The sensitivity of the samples decreases in the order sample GII >sample GI >sample GIII for ethanol vapors. The sensitivity of sample GII for other reducing gases such as CH_4, LPG and CO was also investigated at different operating temperatures. As one can be seen from Fig. 4, the sensitivity of this is remarkably higher for ethanol than for other gases. To secure a good reproducibility of the sensitivity-temperature characteristics, the resistance was measured during cooling the sample after being heated sufficiently at high temperature. It is clear that this material is the most sensitive to ethanol gas and less sensitive to other test gases. The resistance of all the samples was decreased in the presence of reducing gases indicating its n-type semiconductor nature. An n-type behavior of $CoFe_2O_4$ is due to the presence of Fe^{2+} and conductivity was predominantly due to hopping of electrons from Fe^{2+} to Fe^{3+} [18]. D.Y.Lee *et. al* reported that the main conduction mechanism in iron excess ferrite was electron hopping from Fe^{2+} to Fe^{3+} ion, and the main conduction mechanism in Co^{3+} excess ferrite whole hopping from Co^{2+} to Co^{3+} [19].

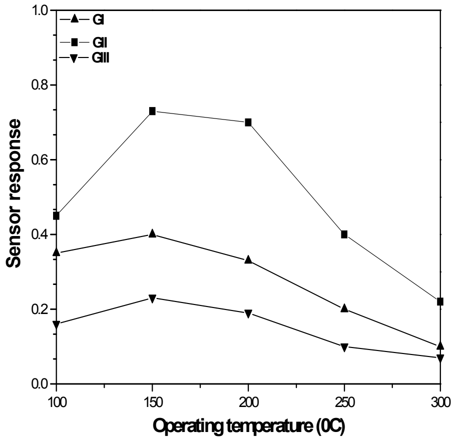

Fig. 3. Sensor responses of samples GI, GII and GIII as a function of temperature (^0C)

3.3 Gas sensing characteristics of Pd impregnated $CoFe_2O_4$

The impregnation of noble metals like Pd, Ag and Au may create additional active sites for the adsorption of the gas or some time may destroy some of the existing active sites depending upon the concentration of additives. With the intention of increasing the surface area, the material being synthesized in the form of nanocrystals and the Pd sensitization is being done to increase its sensitivity. Since the sample G-II showed better characteristics among all other materials further studies were carried on this material by impregnation of 0.5, 1 and 1.5 wt. % Pd over it. After impregnation with Pd, the surface structure has changed quite a bit, introducing more sort of porosity perhaps giving more active sites for the adsorption of gas resulting in better sensitivity.

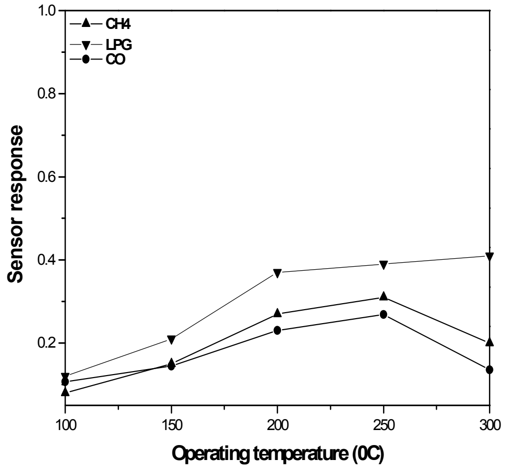

Fig. 4 Sensor response of sample GII to CO, CH_4 and LPG gases as a function of temperature (^0C)

Fig. 3 shows sensor response of Pd impregnated sample GII. The sample GII:1 wt.% Pd has excellent sensitivity to ethanol at the reduced temperature of 100^0C. It can be seen that, the sensitivity of sample with 0.5 and 1.5 wt.% Pd is less than 50%. The Pd as an additive has shown to effectively influence the semiconductive properties of sensor material. The increased sensitivity of sample GII by incorporation of 1 wt.% Pd may be due to creation of more active sites on the surface of sample GII. Two types of interactions between additives and semiconductor may be distinguished. The first is a chemical interaction by which additives assist the redox the redox process of semiconductor oxides. The second interaction is an electronic one in which additives interacts electronically with a semiconductor as a sort of electron donor or acceptor. It is known that the contact of certain metals with semiconductor surfaces produces a Schottky barrier. An electronic interaction in between semiconductor and additives cause a change in surface conductivity of the sensor and hence the conductivity.

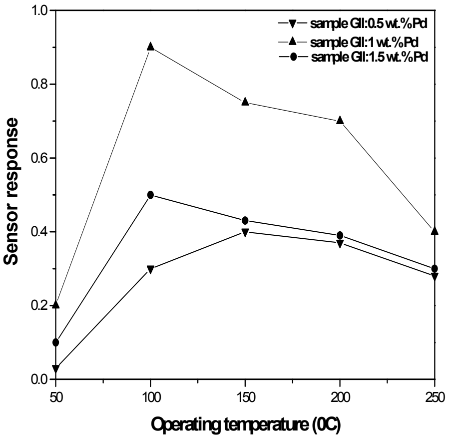

Fig. 5 Sensor response of sample GII impregnated with 0.5, 1 and 1.5 wt.% Pd for ethanol as a function of temperature (^0C)

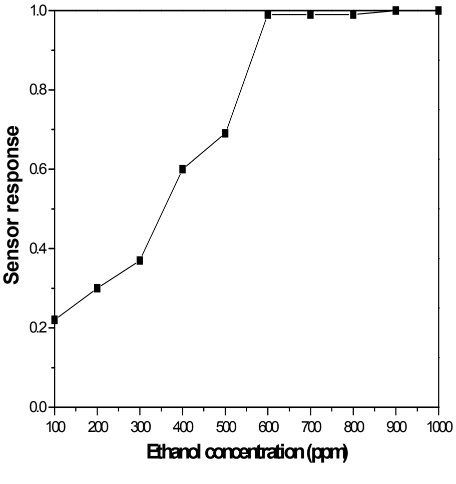

Fig. 6 Sensor response vs. concentration of ethanol in air at 100^0C for the sample GII:1 wt.% Pd

Fig. 4 Shows the sensor response of sample GII:1 wt.% Pd sensor as a function of ethanol in air at 100^0C. The sensor response increases with increase in ethanol concentration and shows saturation at around 600 ppm. At 100^0C, the sensor element is able to detect ethanol even up to 100 ppm with the sensitivity of 0.22.

3.4 Ethanol sensing mechanism

When a sensor thick film is exposed to air, physisorbed oxygen molecules receive electrons from the conduction band of the film and change to $O_{(ads)}^-$ $O_{2(ads)}^-$ and $O_{(ads)}^{2-}$ species. Desorption these species results in decrease or increase of the conductance of the sensor element depending on the nature of gas. The reaction kinematics will proceed as follows:

$O_{2(gas)} \leftrightarrow O_{2(ads.)}$

$O_{2(ads.)} + e^- \leftrightarrow O_{2(ads.)}^-$

$O_{2(ads.)}^- + e^- \rightarrow 2O_{(ads.)}^-$

Sensor conductivity increases when the incoming gas is of reducing type. The reaction between ethanol and ionic species takes place by two different ways:

$C_2H_5OH_{(gas)} + O^- \leftrightarrow CH_3CHO + H_2O + e^-$

$C_2H_5OH_{(gas)} \leftrightarrow C_2H_5O_{(surface)} + H$

$C_2H_5O_{(surface)} \leftrightarrow H + CH_3CHO$

$CH_3CHO + O_{(bulk)} \rightarrow CH_3COOH + O_{(vacancies)}$

4. Conclusions

Nanocrystalline $CoFe_2O_4$ powders were successfully synthesized by polymerizable complex route and their gas sensing properties were investigated. From the results, some conclusions can be drawn as follows-

a) XRD and SEM results showed that polymerizable complex route adopted for material synthesis affected the grain size, grain shape and degree of agglomeration to a large extent.

b) Among the samples GI, GII and GIII, sample GII showed large response to ethanol with relatively good sensitivity at 150^0C.

c) Sample GII impregnated with 1 wt.% Pd exhibited higher sensitivity for ethanol at 100^0C. Impregnation of Pd to sample GII results in drop of temperature from 150 to 100^0C.

A probable ethanol sensing mechanism is suggested based upon the present investigation and reported work. Sample GII:1 wt.% Pd looks to be more promising and efficient ethanol sensor.

References

[1] O. K. Varghese, L. K. Malhotra, G. L. Sharma 1991, Sensors and Actuators B, **55**, 161 (1999).

[2] G. Korotchenkov, V. Brynzari, S. Dmitriev, Sensors and Actuators B, **54**, 197 (1999).

[3] Y. Zhao, Z. Feng, Y. Liang, Sensors and Actuators B, **56**, 224 (1999).

[4] J. R. Brown, P. W. Haycock, L. M. Smith, A. C. Jones, E. W. Williams, Sensors and Actuators B, **63**(1-2), 109 (2000).

[5] S. I. Rembeza, E. S. Rembeza, T. V. Svistova, O. L. Borsiakova, Phys. Stat. Sol. A, **179**(1), 147 (2000

[6] E. Traversa, S. Matsushima, G. Okada, Y. Sadaoka, Y. Sakai, K. Watanabe, Sensors and Actuators B **25**, 661 (1995).

[7] Y. Sadaoka, H. Aono, E. Traversa, M. Sakamoto, Journal of Alloys and Compounds, **278**, 135 (1998).

[8] G. N. Chaudhari, J. Optoelectron. Adv. Mater. **9**(7), 2270 (2007).

[9] Y. Yokomizo, S. Uno, M. Hirata, H. Hiraki, Sens.Actuators, **4**, 599 (1983).

[10] T. Nitta in Chemical sensor technology, vol. 1, ed. by T.Seiyama. Kodansha-Elsevier, New York, 1988, 57.

[11] Z. V. Marinkovic, L. Mancic, R. Maric, O. Milosevic, J. Euro. Ceram. Soc. **21**, 2051 (2001).

[12] T. A. S. Ferreira, J. C. Waerenbourgh, M. H. R. M. Mendonca, M. R. Nunes, F. M. Costa, Solid State Sciences **5**, 383 (2003).

[13] S. Pokhrel, B. Jeyaraj, K. S. Nagaraja, Mater. Lett. **4378**, 1 (2003)

[14] X. Cao, L. Gu, Spindly cobalt ferrite nanocrystals: preparation, characterization and magnetic properties, Nanotechnology **16**, 180 (2005).

[15] N. Keller, C. Pham-Huu, T. Shiga, C. Estourn`es, J.-M. Gren`eche, M. J. Ledoux, J. Magnetism Magnetic Mater. **272–276**, 1642 (2004).

[16] G. B. Ji, S. L. Tang, S. K. Ren, F. M. Zhang, B. X. Gu, Y. W. Du, J. Crystal Growth **270**, 156 (2004).

[17] Y. Tamaura, M. Tabata, Complete reduction of carbon dioxide to carbon using cation-excess magnetite, Nature **346**, 255 (1990).

[18] S. S. Bellad, C. H. Bhosale, Thin Solid Films **322**, 93 (1998).

[19] D. Y. Lee, D. Kim, K. H. Kim, J. S. Choi, Bull. Korean Chem. Soc. **9**, 333 (1988).

---

*Corresponding author: mjpawar@hotmail.com